

See discussions, stats, and author profiles for this publication at: <https://www.researchgate.net/publication/231274153>

Solids Deposition during “Cold Flow” of Wax –Solvent Mixtures in a Flow-loop Apparatus with Heat Transfer

ARTICLE *in* ENERGY & FUELS · JUNE 2009

Impact Factor: 2.79 · DOI: 10.1021/ef900224r

CITATIONS

20

READS

178

2 AUTHORS, INCLUDING:



Anil K Mehrotra

The University of Calgary

160 PUBLICATIONS 2,348 CITATIONS

SEE PROFILE

Solids Deposition during “Cold Flow” of Wax–Solvent Mixtures in a Flow-loop Apparatus with Heat Transfer

Hamid O. Bidmus and Anil K. Mehrotra*

Department of Chemical and Petroleum Engineering, University of Calgary, Calgary, Alberta, Canada T2N 1N4

Received March 14, 2009. Revised Manuscript Received May 3, 2009

“Cold flow” refers to the pipeline flow of a “waxy” crude oil at a temperature, which is below its wax appearance temperature (WAT) and above its pour point temperature (PPT), whereby precipitated wax crystals remain suspended in the flowing crude oil. It has been suggested as an alternative technology for decreasing solids deposition (Merino-Garcia, D.; Corra, S. *Pet. Sci. Technol.* **2008**, *26*, 446). An experimental investigation was undertaken to study solids deposition under cold flow in a flow-loop apparatus, incorporating a small double-pipe heat exchanger. The experiments were performed using 3 and 6 mass % mixtures of a petroleum wax dissolved in Norpar13 (a paraffinic solvent comprising C₉–C₁₆) at different wax–solvent mixture temperatures, T_h , and two flow rates over a deposition time of 1 h. Two sets of deposition experiments were performed: cold flow with $\{WAT \geq T_h > PPT\}$ and “hot flow” with $\{T_h > WAT\}$. The deposit mass decreased with a decrease in wax concentration and with an increase in the coolant temperature. However, the deposit mass decreased with a decrease in the mixture temperature, under cold flow, but it increased with a decrease in the mixture temperature, under hot flow. Also, the deposit mass, under cold flow, was not affected by flow rate. Predictions from a pseudosteady-state heat-transfer model were in good agreement with experimental results, indicating the deposition process to be thermally driven. The liquid–deposit interface temperature in all cases was equal to the WAT of the liquid phase. Variations in both the wax content and the carbon number distribution in deposit samples are discussed.

Introduction

Wax deposition from crude oils is a problem encountered in all sectors of the petroleum industry, ranging from production, to pipeline transportation, to downstream process operations. The presence of deposited “waxy” solids causes a partial or complete blockage of pipelines and equipment involved in these operations. This leads to a reduction of oil flow rate together with an increased pressure drop in flow lines. Furthermore, the efficiency of the processes is affected considerably, leading to substantial expenditures for the control and remediation of solids deposition.

Paraffin waxes are the major constituents of solid deposits from waxy crude oils. Waxes are essentially mixtures of long-chain hydrocarbons with carbon numbers ranging from 18 to 65.² They have a low solubility in crude oil at reduced temperatures that causes them to crystallize and deposit on the cooler surfaces of pipelines and process equipment. Wax particles start to crystallize when the crude oil temperature falls below the wax appearance temperature (WAT). The WAT is the highest temperature at which the first crystals of wax start to appear when a waxy crude oil is cooled. Bhat and Mehrotra³ measured the WAT of several waxy mixtures, while the wax disappearance temperature (WDT) was recorded during heating of the same samples. It was shown that the WDT, rather than the WAT, is closer in value to the thermodynamic liquidus temperature of wax–solvent mixtures.³

Wax deposits consist of liquid and solid phases in a gel-like structure. The composition and relative proportions of liquid and solid phases vary across the deposit thickness. Visual observations of wax deposits under a cross-polarized microscope showed them to consist of platelet-shaped wax crystallites that overlap and interlock around the liquid phase.⁴ Upon further cooling of the crude oil below the pour point temperature (PPT), additional wax precipitation leads to the manifestation of time-dependent rheological behavior in the crude oil.⁵ Waxy mixtures exhibit non-Newtonian rheology at temperatures below the PPT as well as a considerable increase in the apparent viscosity.^{5,6}

The deposit layer formed is exposed to variations in concentration, temperature, and shear rate (due to the flowing crude oil) across its thickness. These factors have been shown to play important roles during deposit formation in tubes or pipelines.^{7–19}

(4) Holder, G. A.; Winkler, J. J. *Inst. Pet.* **1965**, *51*, 228.

(5) Wardhaugh, L. T.; Boger, D. V. *AIChE J.* **1991**, *37*, 871.

(6) Tiwary, D.; Mehrotra, A. K. *Can. J. Chem. Eng.* **2004**, *82*, 162.

(7) Singh, P.; Venkatesan, R.; Fogler, H. S.; Nagarajan, N. *AIChE J.* **2000**, *46*, 1059.

(8) Singh, P.; Venkatesan, R.; Fogler, H. S.; Nagarajan, N. *AIChE J.* **2001**, *47*, 6.

(9) Singh, P.; Youyen, A.; Fogler, H. S. *AIChE J.* **2001**, *47*, 2111.

(10) Creek, J. L.; Lund, H. J.; Brill, J. P.; Volk, M. *Fluid Phase Equilib.* **1999**, *80/1*, 158.

(11) Mehrotra, A. K.; Bhat, N. V. *Energy Fuels* **2007**, *21*, 1277.

(12) Patton, C. C.; Casad, B. M. *Soc. Pet. Eng. J.* **1970**, *10* (1), 17.

(13) Bott, T. R.; Gudmunsson, J. S. *Can. J. Chem. Eng.* **1977**, *55*, 381.

(14) Ghedamu, M.; Watkinson, A. P.; Epstein, N. Mitigation of Wax Buildup on Cooled Surfaces, In *Fouling Mitigation of Industrial Heat-Exchange Equipment*; Panchal, C. B., Bott, T. R., Somerscales, E. F. C., Toyama, S., Eds.; Begel House: New York, 1997, p 473–489.

(15) Jennings, D. W.; Weispfennig, K. *Energy Fuels* **2005**, *19*, 1376.

(16) Wu, C.; Wang, K. S.; Shuler, P. J.; Tand, Y.; Creek, J. L.; Carlson, R. M.; Cheung, S. *AIChE J.* **2002**, *48*, 2107.

* Corresponding author. Phone: (403) 220-7406; fax: (403) 284-4852; e-mail: mehrotra@ucalgary.ca.

(1) Merino-Garcia, D.; Corra, S. *Pet. Sci. Technol.* **2008**, *26*, 446.

(2) Srivastava, S. P.; Handoo, J.; Agrawal, K. M.; Joshi, G. C. *J. Phys. Chem. Solids* **1993**, *54*, 639.

(3) Bhat, N. V.; Mehrotra, A. K. *Ind. Eng. Chem. Res.* **2004**, *43*, 3451.

An increase in the wax concentration of a crude oil results in a higher WAT, which increases the extent of deposited solids.²⁰ Lower crude oil temperatures (above the WAT) and lower pipe wall temperatures (below the WAT) favor an increase in solids deposition.^{12–19} Likewise, studies have shown that the mass of deposited solids decreases as the flow rate is increased under both laminar and turbulent flow regimes.^{7–19} Thus, a complete description of the deposit-layer formation and growth process would involve a combination of several considerations, such as thermodynamics and solid–liquid multiphase equilibria, heat transfer, fluid dynamics, rheology, and mass transfer.

Several mechanisms have been suggested to be responsible for the formation of deposits from waxy crude oil mixtures.²¹ A commonly accepted mechanism is the molecular diffusion approach,^{7–10,22–25} which is based on the premise that deposition takes place through radial transport of wax molecules induced by a radial concentration gradient. This concentration gradient is caused by the temperature gradient resulting from the difference between the flowing crude oil temperature and the pipe-wall temperature. For modeling wax deposition, this approach assumes a gradual increase of the temperature at the liquid–deposit interface from a value close to the pipe-wall temperature initially to a maximum value equal to the WAT as steady state is attained. It is pointed out that this assumption of a gradually increasing interface temperature has not been validated experimentally.

Other mechanisms that have been considered to explain the wax deposition process include shear dispersion and Brownian diffusion. Wax deposition could occur by shear dispersion through the cross-stream transport of solid particles in suspension. Studies have reported the migration of particles by shear dispersion toward the region between the pipe centerline and the pipe wall.²⁶ Brownian diffusion could also occur in a crude oil with very small wax crystals suspended. In the presence of a concentration gradient of solid crystals, a net transport of wax crystals by Brownian diffusion can occur in the direction of decreasing concentration.

Several studies have been based on an alternative approach that considers wax deposition as a predominantly heat-transfer process involving (partial) freezing or solidification.^{11–14,17–19,27,28} The rate of heat transfer through the deposit layer is dependent on the thermal driving force between the bulk crude oil temperature and the cooler pipe-wall temperature. The energy balance accounts for the latent heat released during phase transformation of the crude oil or wax–solvent mixture at the liquid–deposit interface and within the deposit-layer. Convective and/or conductive thermal resistances due to the flowing crude oil, the pipe wall, insulation, and the surroundings also influence the rate of heat transfer. An assumption made in the heat-transfer approach is that the liquid–deposit interface temperature, T_d , remains equal to the WAT of the crude oil or wax–solvent mixture throughout the deposition process.

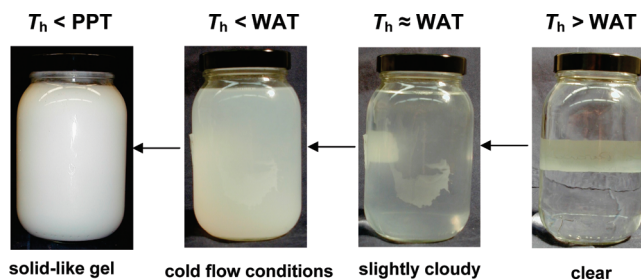


Figure 1. An illustration of stages involved in the cooling of a wax–solvent mixture in a bottle from above WAT to below the PPT.

Laboratory investigations^{17–19,28} have reported a relatively fast attainment of thermal pseudosteady-state during deposition from waxy mixtures flowing under laminar and turbulent conditions. Results obtained from these studies were in good agreement with predictions from a steady-state heat-transfer model, which identified the temperature difference across the deposit layer to be an important parameter in the deposition process. A dimensionless parameter, defined as the ratio of the temperature difference across the deposit layer to the overall temperature difference, was shown to correlate well with the mass of deposited solids.^{17–19,28} This dimensionless parameter, at steady state, was shown to be equal to the fraction of the thermal resistance offered by the deposit layer. Moreover, this parameter is dependent on the average thermal conductivity and thickness of the deposit.

Various techniques have been applied to the control or remediation of wax deposition and these can be grouped into: thermal, mechanical, chemical, and biological methods.^{29–33} However, most of these methods are cost intensive, especially when dealing with long production lines or offshore facilities, and in some cases can lead to increased deposition in process equipment further downstream.³² “Cold flow” is an alternative approach that has been proposed to control and reduce solids deposition problems during the flow of waxy crude oil. This type of flow occurs when a slurry is formed at cooler temperatures, which is transported through the pipeline under stable conditions with no deposition of the solids.¹ Figure 1 shows the gradual changes in the appearance of a wax–solvent mixture that is cooled from above the WAT to below the PPT. The third bottle illustrates typical cold flow conditions in which a waxy crude oil (or a wax–solvent mixture) is between the WAT and PPT. Under these conditions, the flow in a pipeline would occur as a slurry with wax crystals suspended in the crude oil.

Although a limited amount of studies can be found in the literature relating to cold flow as a means of preventing wax deposition, there are numerous patents on methods for creating waxy slurries during this type of flow.¹ Merino-Garcia and Corraera¹ discussed some of these patents in a review of the cold flow technology. Challenges faced by this technology include successfully creating a stable slurry and cooling the mixture to

(17) Bidmus, H. O.; Mehrotra, A. K. *Ind. Eng. Chem. Res.* **2004**, *43*, 791.

(18) Parthasarathi, P.; Mehrotra, A. K. *Energy Fuels* **2005**, *19*, 1387.

(19) Fong, N.; Mehrotra, A. K. *Energy Fuels* **2007**, *21*, 1263.

(20) Hammami, A.; Raines, M. A. *Soc. Pet. Eng. J.* **1999**, *4*, 9.

(21) Azevedo, L. F. A.; Teixeira, A. M. *Petrol. Sci. Technol.* **2003**, *21*, 393.

(22) Majeed, A.; Bringedai, B.; Overa, S. *Oil Gas J.* **1990**, *18*, 63.

(23) Svendsen, J. A. *AIChE J.* **1993**, *39*, 1377.

(24) Kok, M. V.; Saracoglu, R. O. *Pet. Sci. Technol.* **2000**, *18*, 1121.

(25) Ramirez-Jaramillo, E.; Lira-Galeana, C.; Manero, O. *Pet. Sci. Technol.* **2004**, *22*, 821.

(26) Segre, G.; Silberberg, A. *J. Fluid Mech.* **1962**, *14*, 136.

(27) Bhat, N. V.; Mehrotra, A. K. *Ind. Eng. Chem. Res.* **2005**, *44*, 6948.

(28) Tiwary, R.; Mehrotra, A. K. *Energy Fuels* **2009**, *23*, 1299.

(29) Becker, J. R. *Oilfield Paraffin Treatments: Hot Oil and Hot Water compared to Crystal Modifiers*; Proceedings 2000 SPE Ann. Tech. Conf. & Exhib. - Prod. Oper. & Eng. Gen.: Dallas, USA, Oct 1–4, 2000.

(30) Bosch, F. G.; Schmitt, K. J.; Eastlund, B. J. *IEEE Trans. Ind. Applic.* **1992**, *28* (1), 190.

(31) Sarmiento, R. C.; Ribbe, G. A. S.; Azevedo, L. F. A. *Heat Transfer Eng.* **2004**, *25* (7), 2.

(32) Newberry, M. E.; Addison, G. E.; Barker, K. M. *SPE Prod. Eng.* **1986**, *1* (3), 213.

(33) Braden, B. *The Use of Enzymes to Control Paraffin and Asphaltene Deposits in the Wellbore*; Presented at the SPE Western Regional Meeting, California, USA, June 25–27, 1997.

ambient or pipe-wall temperature without any deposition occurring in the process. Deposition of solids is presumed to be reduced during cold flow because of a reduced temperature driving force as well as the preferential crystallization of wax onto the flowing solid slurry that act as nucleation sites.¹ Studies have shown the cold flow technology to be applicable in the prevention of gas hydrate formation during the flow of crude oil and natural gas.³⁴

This study was carried out to provide an improved understanding of the wax deposition process during cold flow conditions. Note that the term “hot flow”, in this study, is used for the deposition experiments in which the wax–solvent mixture temperature is higher than the WAT. A novel bench-scale flow loop apparatus was developed for investigating cold flow deposition from wax–solvent mixtures. An experimental program was undertaken to study the effects of mixture composition, bulk mixture, coolant temperatures, and flow rate on the deposition process. The influence of these factors on the deposited solids was also investigated. All cold flow deposition experiments were performed with the mixture temperature at or below the WAT (giving a suspended solid phase in the liquid phase) and continued until after the attainment of a thermal steady state. The results of this study extend the applicability of the steady state heat-transfer model to solid deposition from wax–solvent mixtures under cold flow conditions.

Heat-transfer Considerations

The steady state heat transfer model has been successfully used to analyze experimental results from wax deposition under laminar and turbulent flow conditions.^{11,17–19,28} When a “hot” wax–solvent mixture flows through a pipe exposed to a coolant or wall temperature below its WAT, the resulting radial temperature gradient causes an outward transfer of thermal energy from the mixture. This leads to the formation of a deposit layer that grows in thickness until reaching a thermal steady state, when the rates of heat transfer across the wax–solvent mixture, deposit layer, pipe-wall, and coolant become the same. That is, at steady state, the deposit layer stops growing and all thermal resistances become constant.

For a wax–solvent mixture flowing under conditions of cold flow and concurrently in a double-pipe heat exchanger, the equality of the rate of heat transfer, q , lost by the mixture, gained by the coolant, and exchanged between both “hot” and “cold” streams is expressed by:

$$q = \dot{m}_h C_h (T_{hi} - T_{ho}) + \dot{m}_h \Delta f \Delta H_m = \dot{m}_c C_c (T_{co} - T_{ci}) - q_{\text{gain}} = U_i A_i \Delta T_{LM} \quad (1)$$

where \dot{m}_h and \dot{m}_c are mass flow rates of the wax–solvent mixture and coolant streams, respectively; C_h and C_c are the average specific heat capacities of the mixture and coolant streams, respectively; T_{hi} and T_{ho} are the inlet and outlet mixture temperatures, respectively; T_{ci} and T_{co} are the inlet and outlet temperatures of the coolant, respectively; Δf is the change in solid (wax) phase fraction; ΔH_m is the latent heat of fusion for wax; U_i is the inside overall heat-transfer coefficient; A_i is the inside pipe (or tube) surface area; ΔT_{LM} is the log-mean average temperature difference between the hot and cold streams; and q_{gain} is the amount of thermal energy gained or lost by the coolant from the surroundings. At a thermal steady state, assuming the deposit layer thickness, x_d , to be uniform, the

equality of heat flux through the four thermal resistances, R_h , R_d , R_m , and R_c , is expressed as follows:

$$\frac{q}{A_i} = \frac{h_h(\bar{T}_h - T_d)}{r_i/(r_i - x_d)} = \frac{k_d(T_d - T_{wi})}{r_i \ln[r_i/(r_i - x_d)]} = \frac{k_m(T_{wi} - T_{wo})}{r_i \ln[r_o/r_i]} = \frac{h_c(T_{wo} - \bar{T}_c)}{r_i/r_o} \quad (2)$$

where h_h and h_c are the individual convective heat-transfer coefficients for the mixture and coolant streams, respectively; x_d is the deposit thickness; k_d and k_m are the thermal conductivities of the deposit layer and the pipe-wall, respectively; T_d is the liquid–deposit interface temperature; T_{wi} and T_{wo} are the inside and outside pipe-wall temperatures, respectively. Experimental data can be used to solve the four equalities in eq 2 simultaneously for the four unknowns of T_{wi} , T_{wo} , T_d , and k_d .

Interface Temperature, T_d . As already mentioned, it is assumed in the heat-transfer approach for modeling wax deposition, that the liquid–deposit interface temperature, T_d , remains constant and equal to the WAT of the wax–solvent mixture throughout the deposition process. This was confirmed experimentally to be valid for deposition at thermal steady state, for both laminar and turbulent flow conditions.^{17–19,28} Bidmus and Mehrotra^{35,36} recently reported experimental results for T_d during wax deposition from prepared wax–solvent mixtures under static and sheared cooling. The results indicated that T_d , during deposit-layer growth remained constant at the WAT of the liquid phase.^{35,36} Furthermore, the measured T_d was found to be about 1–2 °C below the mixture temperature when the wax–solvent mixture temperature, T_h , fell below the WAT (giving rise to wax crystals suspended in the liquid phase as is the case with cold flow). The T_d decreased with the mixture temperature, T_h , when T_h was less than WAT and was found to be equal to the new effective WAT of the liquid phase.³⁶

Fractional Deposit Thermal Resistance, θ_d . The combined thermal resistance is expressed in terms of the four individual thermal resistances and the overall heat transfer coefficient, as follows:

$$\frac{2\pi L}{U_i A_i} = \frac{1}{(r_i - x_d)h_h} + \frac{\ln[r_i/(r_i - x_d)]}{k_d} + \frac{\ln[r_o/r_i]}{k_m} + \frac{1}{r_o h_c} \quad (3)$$

Bidmus and Mehrotra¹⁷ proposed a dimensionless parameter, θ_d , as the ratio of the thermal resistance of the deposit layer to the combined thermal resistance:

$$\theta_d = \frac{R_d}{R_h + R_d + R_m + R_c} = \frac{T_d - T_{wi}}{T_h - T_c} \quad (4)$$

As shown in eq 4, θ_d also represents the ratio of the temperature drop across the deposit layer to the overall thermal driving force at steady state. Similar ratios can be obtained for the other three thermal resistances to give θ_h , θ_m , and θ_c .³⁷

Calculations were performed over the range of typical cold flow experimental conditions in this study to show the effect of the deposit-layer thickness, x_d , on θ_h , θ_d , θ_m , and θ_c . In these calculations, T_d was assumed to be 1 °C below the mixture temperature, T_h , for the cold flow conditions. A comparison of

(35) Bidmus, H.; Mehrotra, A. K. *Energy Fuels* **2008**, *22*, 1174.

(36) Bidmus, H.; Mehrotra, A. K. *Energy Fuels* **2008**, *22*, 4039.

(37) Bidmus, H. O. Investigation of Solids Deposition from Wax-Solvent Mixtures under Static, Sheared, and ‘Cold Flow’ Cooling Conditions; PhD Thesis, University of Calgary, Calgary, Canada, 2009.

(34) Gudmunsson, J. S. *Cold Flow Hydrate Technology*; 4th International Conf. Gas Hydrates: Yokohama, Japan, May 19–23, 2002.

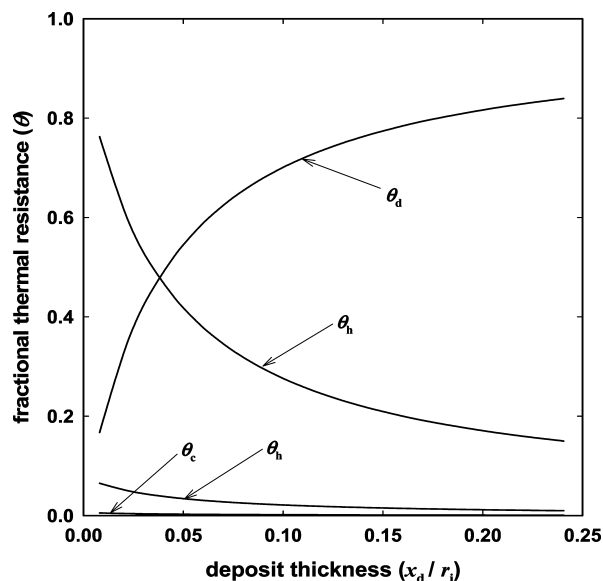


Figure 2. Predictions for the variation of the fractional thermal resistances with changes in the deposit layer thickness during cold flow.

the magnitudes of all the four thermal fractional resistances is shown in Figure 2. For a small deposit thickness ($x_d/r_i < 0.04$), the convective thermal resistance due to the wax–solvent mixture, θ_h , is the predominant resistance. The deposit layer offers the dominant thermal resistance when $x_d/r_i > 0.04$. This indicates that, at this point, the largest temperature drop would be across the deposit layer. The relative contributions of the thermal resistances due to the coolant and the tube wall, θ_c and θ_m , are predicted to be negligible for all deposit thicknesses; hence, an uncertainty in these did not impact the deposition calculations appreciably.

Experimental Section

Materials. All cold flow deposition experiments were carried out with prepared mixtures of a paraffinic wax in a petroleum solvent; the results obtained could be validated with crude oil samples in future investigation. It is noted that studies using similar prepared mixtures have been carried out previously in our laboratory to investigate wax deposition under laminar and turbulent conditions.^{17–19,28}

The wax sample used was Parowax, which was obtained from Conros Corp (Ontario, Canada) in the form of small pellets. This wax was also used in two previous studies for wax deposition under turbulent flow.^{19,28} It comprised of *n*-alkanes over the range of C_{20} to C_{50} with an average molar mass of $414.2 \text{ kg kmol}^{-1}$, which is equivalent to a mean carbon number of about 29. Parowax has a melting point range and density (at 23°C) of $57\text{--}62^\circ\text{C}$ and 915 kg m^{-3} , respectively. Norpar13, obtained from Imperial Oil (Ontario, Canada), was used as solvent for preparing the wax–solvent mixtures. Norpar13 consisted of *n*-alkanes ranging from C_9 to C_{16} , with a density of 754 kg m^{-3} at 23°C .^{3,18,19,28,35,36} The average molar mass of Norpar13 was calculated to be $185.7 \text{ kg kmol}^{-1}$, which corresponds to an average carbon number of about 13. The carbon number distributions of Parowax and Norpar13 are shown in Figure 3. Parowax and Norpar13 do not show an overlap in their carbon number distributions, which as explained later was essential for estimating the compositional changes in the deposit layer on a solvent-free basis.

WAT and PPT Measurements. Parowax–Norpar13 mixtures with wax concentrations of 3, 6, and 20 mass % were prepared. The WAT and PPT of these mixtures were measured using a visual method with cooling in steps of 1°C .^{3,6,17–19,28,35–37} The highest temperature at which wax crystals were first observed visually was

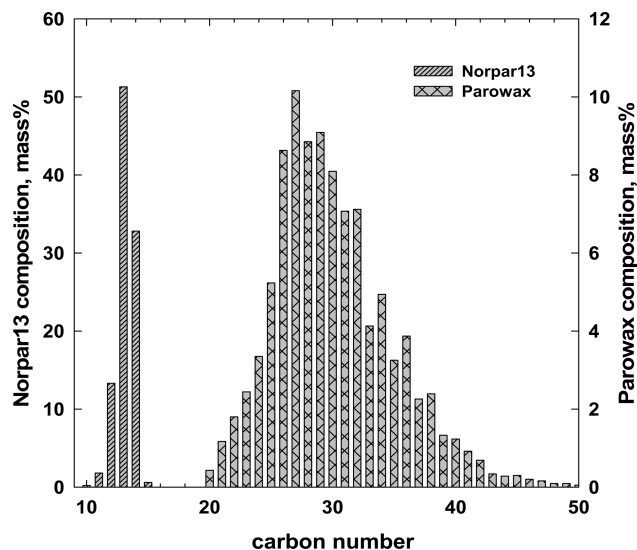


Figure 3. Carbon number distributions of Norpar13 and Parowax.¹⁹

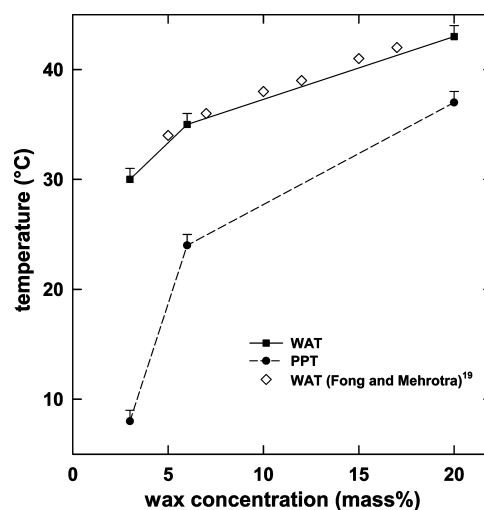


Figure 4. WAT and PPT values for Parowax–Norpar13 mixtures.

taken to be the WAT, while that at which the sample ceased to flow, when held horizontally in a pour point tube, was taken to be the PPT.³ Figure 4 compares the measured WAT and PPT values for the prepared Parowax–Norpar13 mixtures. In this figure, the measured WAT values are shown to compare well with those reported by Fong and Mehrotra.¹⁹ It is observed that the difference between the WAT and PPT values increases as the wax concentration is reduced. The error bars in Figure 4 indicate the uncertainty associated with the WAT and PPT measurements, which is up to $\pm 1^\circ\text{C}$.

Flow-loop Apparatus for Cold Flow Deposition. A bench-scale flow-loop apparatus was designed to carry out the wax deposition experiments under conditions of cold flow. The flow-loop consisted of a double-pipe heat exchanger (operated cocurrently), three temperature-regulated heating/cooling baths, an 8.7 L plexiglass reservoir, a centrifugal pump, a flowmeter, a valve for regulating the wax–solvent mixture flow rate, a vent valve for aiding drainage during shut-down, and T-type thermocouples connected to a data-logger. A schematic of the experimental setup is shown in Figure 5.

The primary means for cooling the wax–solvent mixture was cold air, which was bubbled through two air stones placed at the bottom of the reservoir holding the wax–solvent mixture. Without a contact surface, this technique helped in creating wax crystals suspended in the liquid mixture. However, the rate of cooling with cold air was found to be inadequate, especially to offset the thermal energy generated due to the recirculation of the mixture via the centrifugal pump. To increase the cooling capacity, the reservoir

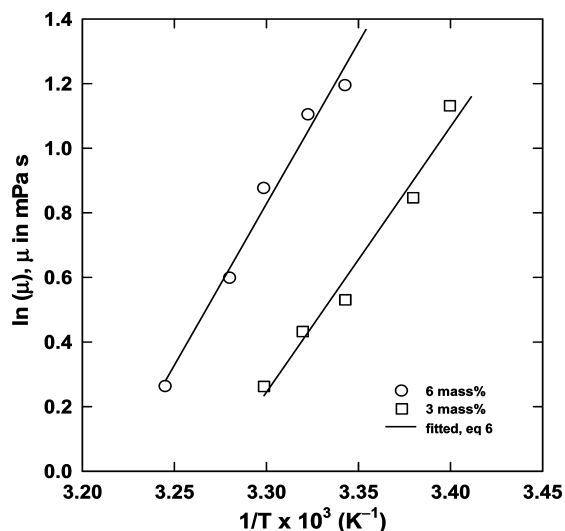


Figure 6. Apparent viscosities of 3 and 6 mass % Parowax–Norpar13 mixtures under conditions of cold flow.

Table 2. Viscosity Regression Constants for Equation 6

wax concentration (mass %)	constants in viscosity correlation, eq 6	
	b_1	b_2
3	-26.90 ± 0.09	8226 ± 26
6	-32.14 ± 0.11	9991 ± 35

experiments was found to be 8.9%. It was observed that the predictions for the deposited solids from the heat transfer model were not significantly affected by an uncertainty in h_h or h_c ,^{17–19} hence, eq 5 was used for estimating the heat transfer coefficients in all calculations.

Apparent Viscosity of Parowax–Norpar13 Mixtures. Cold flow involves the flow of a slurry-like mixture exhibiting non-Newtonian characteristics. The viscosity of wax–solvent mixtures was measured with a rotational-type concentric cylinder viscometer, obtained from ThermoFisher Scientific (Ontario, Canada) at temperatures between their respective WAT and PPT.

Results obtained from the viscometer measurements are shown in Figure 6 where apparent viscosity data are presented for both Parowax–Norpar13 mixtures over a temperature range of WAT and WAT – 10 °C. In this figure, the natural logarithm of the viscosity is plotted against inverse temperature data. It is observed that as the concentration of wax in the mixture increases, the viscosity of the mixture also increases. The viscosity data for both wax–solvent mixtures were fitted to the following equation:

$$\mu = 10^3 \times \exp[b_1 + b_2/(T_h + 273.15)] \cdot (WAT - 10) \leq T_h \leq WAT \quad (6)$$

The regression constants b_1 and b_2 in eq 6, obtained for both concentrations of the wax–solvent mixtures, are given in Table 2. Equation 6 was used in the heat transfer calculations for the cold flow deposition experiments. For the hot flow experiments, with the wax–solvent mixture temperature (T_h) greater than WAT, the viscosity correlations given by Fong and Mehrotra¹⁹ were used.

Results and Discussion

Results from the cold flow deposition experiments, carried out according to a factorial design of experiments, are presented and discussed in the following sections. The amount of deposited solids was expressed in terms of the mass of deposit per unit inside tube surface area (Ω), and the results are compared with predictions from heat transfer considerations.

Thermal Steady State. To predict the amount of deposited solids during cold flow using steady-state heat transfer consid-

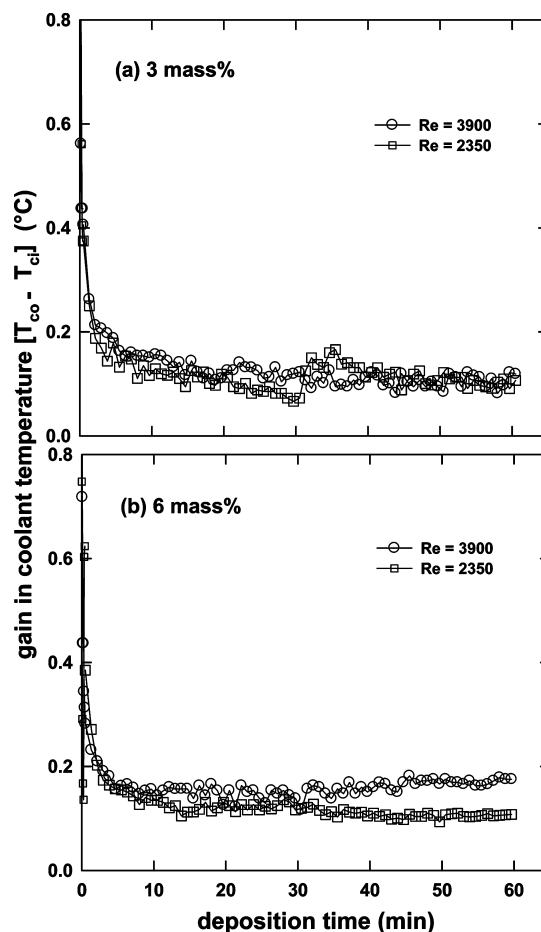


Figure 7. Approach to thermal steady state during cold flow deposition evidenced by the difference in coolant temperatures for 1 h experiments at $T_h = WAT$.

erations, it was necessary to ensure that each experiment attained a thermal steady state before termination. Previous deposition experiments carried out with similar paraffinic mixtures under laminar and turbulent flow showed a thermal steady state was reached within 30 min.^{17–19,28} Experimental data for the gain in coolant temperature ($T_{co} - T_{ci}$) with time are shown in Figure 7 for the experiments carried out at $T_h = WAT$. The results are presented for both wax–solvent mixtures at different flow rates or Reynolds number. The results indicate that ($T_{co} - T_{ci}$) was initially high but then decreased to reach a thermal steady state in about 15 min. The temperature profiles also do not show any significant variation of ($T_{co} - T_{ci}$) with Reynolds number. Similar results were obtained for all other deposition experiments.³⁷ The results presented in Figure 7 provide support for use of the steady-state heat transfer model for wax deposition during cold flow as used in this study.

Difference between Mixture and Interface Temperatures. As previously mentioned, the interface temperature, T_d , decreases with mixture temperature, T_h , when $T_h \leq WAT$.^{35–37} Equations 1 and 2 were solved using the data obtained from the cold flow deposition experiments to calculate the wall temperatures, T_{wi} and T_{wo} , the average deposit thermal conductivity, k_d , and the interface temperature, T_d .

In Figure 8, results for the interface temperature, T_d , are compared with the mixture temperature, T_h , for the experiments carried out with a mixture flow rate of 10 L min^{–1}. The results, which also include those from the hot flow experiments, show that T_d was close to the mixture WAT when $T_h > WAT$. However, when $T_h = WAT$, T_d became lower than the WAT. These trends were observed in the experiments with a flow rate

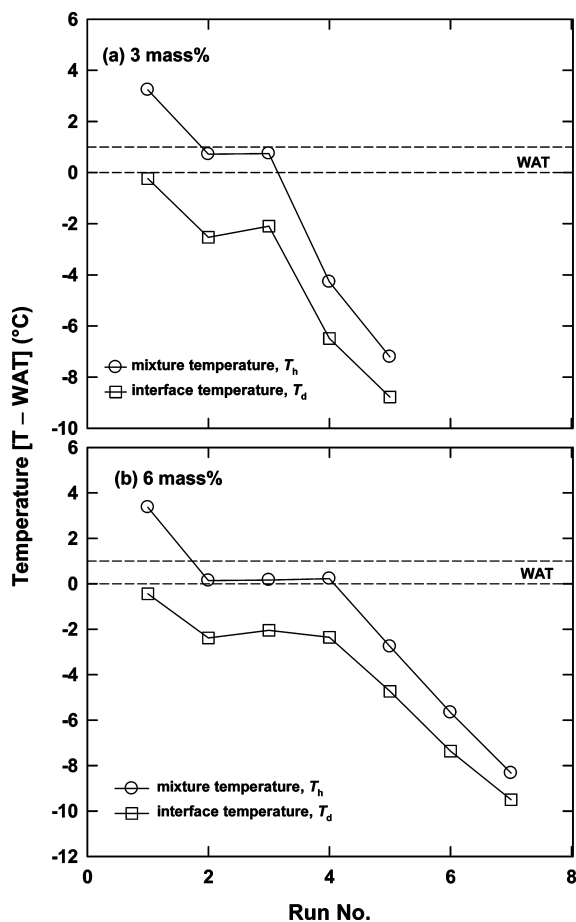


Figure 8. Effect of change in mixture temperature on the interface temperature at flow rate of 10 L min^{-1} for (a) 3 mass % wax-solvent and (b) 6 mass % wax-solvent mixtures.

of 6 L min^{-1} .³⁷ An interesting observation in Figure 8 is that the temperature profiles for both T_h and T_d are nearly parallel below the WAT. Accordingly, a parameter, δ_{WAT} , was defined as follows.

$$\delta_{\text{WAT}} = T_h - T_d; \quad (T_h \leq \text{WAT}) \quad (7)$$

That is, δ_{WAT} is defined as the difference between T_h and T_d when the mixture temperature, T_h , falls below its WAT.

Deposit Properties (T_d , δ_{WAT} , and k_d). Average values of the interface temperature, T_d , the deposit thermal conductivity, k_d , and δ_{WAT} were calculated from eqs 1, 2, and 7 for all deposition experiments. These calculated values are presented in Table 3. Average values of T_d are provided in Table 3 for only hot flow experiments since, as shown in Figure 8, the cold flow T_d values changed with T_h . It is observed that the hot flow T_d values are essentially the same as the experimentally measured WAT for both concentrations of wax-solvent mixture. This is in agreement with previous hot flow studies under laminar and turbulent flows.^{17–19,28} Due to the varying T_d values, average δ_{WAT} values are instead presented for the cold flow experiments. As shown in Figure 8, $\delta_{\text{WAT}} = (T_h - T_d)$ was relatively constant for each mixture composition. Average values calculated for k_d are reported in Table 3 for both cold flow and hot flow experiments.

The average k_d values are almost the same for the different wax concentrations during deposition in each type of flow. However, the k_d values obtained during cold flow are lower than those obtained from the hot flow experiments. It is pointed out that, for the same flow rate, the Reynolds number for the cold

flow experiment was lower than that for the hot flow experiment; this was because of a variation in viscosity of the wax-solvent mixtures over the range of T_h for both types of flow. Previous studies have shown that k_d values at higher Reynolds numbers or under turbulent flow are higher than those obtained at lower Reynolds numbers or under laminar flow.^{18,19} The T_d values in Table 3 for the hot flow experiments are within the range of those obtained in previous deposition studies.^{17–19,28} Furthermore, these results show that T_d can be assumed to be equal to WAT in heat transfer calculations for hot flow, as shown previously.^{17–19,28} Both wax-solvent mixtures gave an average δ_{WAT} value of about 2.2°C . The average δ_{WAT} value was used to estimate the interface temperature, T_d , in the heat transfer calculations for cold flow experiments.

Effect of Wax-Solvent Mixture Temperature, T_h . The mass of deposit per unit surface area, Ω , obtained from all the deposition experiments are plotted against $(T_h - \text{WAT})$ in Figure 9. Note that this figure includes both sets of deposition results, that is, the experiments carried out at $T_h > \text{WAT}$ (hot flow experiments) and at $T_h \leq \text{WAT}$ (cold flow experiments). Predictions obtained with selected values of the deposit thermal conductivity, k_d , from the heat-transfer model are presented as smooth curves for both the cold flow and hot flow deposition experiments. The region between the vertical dotted lines in each plot represents the $\pm 1^\circ\text{C}$ uncertainty in WAT measurements. The WAT also separates the cold flow results on the left from the hot flow results on the right.

Results from the hot flow experiments indicate that the deposit mass increased with a decrease in the wax-solvent mixture temperature, T_h . That is, a larger deposit mass occurs even though the overall thermal driving force, $(T_h - T_c)$, is decreased. Similar trends were also reported in previous deposition studies involving hot flow experiments.^{17–19,28} On the other hand, results from the cold flow experiments, with $T_h < \text{WAT}$, indicate an opposite trend; that is, the mass of deposit decreases with a decrease in T_h . It is pointed out that the temperature difference between the liquid-deposit interface and the coolant or tube wall, $(T_d - T_c)$, is an important parameter for the mass of deposit.^{20,21} However, the interface temperature, T_d , was constant during hot flow deposition, whereas it decreased with a lowering of T_h (due to the precipitation of wax crystals) during cold flow deposition. Thus, the different trends observed during deposition for both types of flow are attributed to changes in the liquid-deposit interface temperature, T_d .

Furthermore, it is observed in Figure 9 that the mass of deposit and the mixture temperature, T_h , for the cold flow experiments are related linearly but are not for the hot flow experiments. In both flow types, the maximum amount of deposition is observed to occur as T_h approaches WAT of the original wax-solvent mixture.

Significance of δ_{WAT} . Deposition experiments in the absence of a thermal driving force produced negligible to zero amounts of deposited solids.^{7,17,27,38} Therefore, it was anticipated that no deposition would occur during cold flow when the mixture temperature, T_h , became equal to the coolant temperature, T_c . However, the cold flow results in Figure 9 indicate that the mass of deposit is zero when T_h is higher than T_c by about 2°C . This temperature difference is the same as the average δ_{WAT} value obtained for both mixtures, which suggests that the mass of deposit becomes zero when the interface temperature, T_d (given by $T_d = T_h - \delta_{\text{WAT}}$) becomes equal to the coolant temperature, T_c . Note that the temperature difference ratio, θ_d , at this point

(38) Burger, E. D.; Perkins, T. K.; Striegler, J. H. H. *J. Petrol Technol.* **1981**, 6, 1075.

Table 3. Liquid–Deposit Interface Temperature (T_d), δ_{WAT} , and Average Deposit Thermal Conductivity (k_d) Estimated from All Deposition Heat Transfer Data

Parowax–Norpar13 mixture	measured WAT (°C)	average estimated T_d (°C)	average estimated δ_{WAT} (°C)	average estimated k_d (W m ⁻¹ K ⁻¹)
3 mass % (hot flow)	30 ± 1	29.8 ± 0.3		0.29 ± 0.09
6 mass % (hot flow)	35 ± 1	34.6 ± 0.5		0.32 ± 0.04
3 mass % (cold flow)			2.2 ± 0.8	0.17 ± 0.05
6 mass % (cold flow)			2.2 ± 0.5	0.19 ± 0.03

(approximately equal to $\{T_d - T_c\}/\{T_h - T_c\}$) also becomes equal to zero. These observations indicate that a difference between T_d and T_c , with $T_d > T_c$, is essential for the deposition to occur.^{17–19} In other words, no deposition would occur during cold flow when $T_h = (T_c + \delta_{WAT})$ or $T_d \approx T_c$.

Effect of Mixture Composition and Re. A comparison of the results in Plots (a) and (b) of Figure 9 reveals the effect of the wax–solvent mixture composition on deposition under cold flow conditions. The results show that an increased deposition occurs at the higher wax concentration of 6 mass % than the 3 mass % wax–solvent mixture for similar values of $(T_h - WAT)$ and $(WAT - T_c)$. The results also show that the average deposit thermal conductivity for the 6 mass % mixture is slightly higher, as supported by the results in Table 3. However, for the hot flow experiments, the wax concentration does not significantly affect the amount of deposit for similar values of $(T_h - WAT)$ and $(WAT - T_c)$.

As indicated in Figure 9, the Reynolds number varied considerably at each flow rate (6 and 10 L min⁻¹) due to a variation in viscosity over the range of T_h covering both hot flow and cold flow. The results from the cold flow experiments, in particular, did not show any noticeable effect of the mixture flow rate, F_h , or the Reynolds number, Re, on the amount of deposit. The hot flow results, however, are in agreement with previously reported trends that the mass of deposit decreases with an increase in F_h or Re.^{7–10,17–19}

Effect of Coolant Temperature, T_c . In Figure 10, predictions from the heat-transfer model are presented to show the effect

of the coolant temperature, T_c , on wax deposition during cold flow and hot flow. For both types of flow, the deposit mass per unit area increases with a decrease in the coolant temperature, which is attributed to an increase in the thermal driving force for deposition as T_c is lowered. The predictions for cold flow show that no deposition occurred when T_h was slightly higher than T_c . Again, the predicted mass of deposit for each coolant temperature approaches zero as the liquid–deposit interface temperature, T_d , becomes equal to the coolant temperature (i.e., $T_d = T_c = T_h - \delta_{WAT}$).

Fractional Thermal Resistance of the Deposit. All of the deposit mass data obtained from the cold flow deposition experiments with both wax–solvent mixtures are plotted in Figure 11 with respect to the fractional thermal resistance, θ_d , offered by the deposit layer. Predictions from eq 4 were obtained at the three indicated values of the deposit thermal conductivity, k_d . As shown in Figure 11, the mass of deposit increases with an increase in θ_d . The mass of deposit is predicted to be zero at $\theta_d = 0$; i.e., in the absence of any deposit, which as shown previously occurs when $T_d = T_c$. Thus, the predictions from the heat-transfer model agree well with the experimental results. This suggests that the fractional temperature drop across the deposit layer is an important parameter that can also be utilized to predict solids deposition under cold flow of waxy mixtures. The results also show that the mass of deposition, and correspondingly θ_d , increases with an increase in the deposit thermal conductivity, k_d . These observations are similar to those reported previously for hot flow under both laminar and

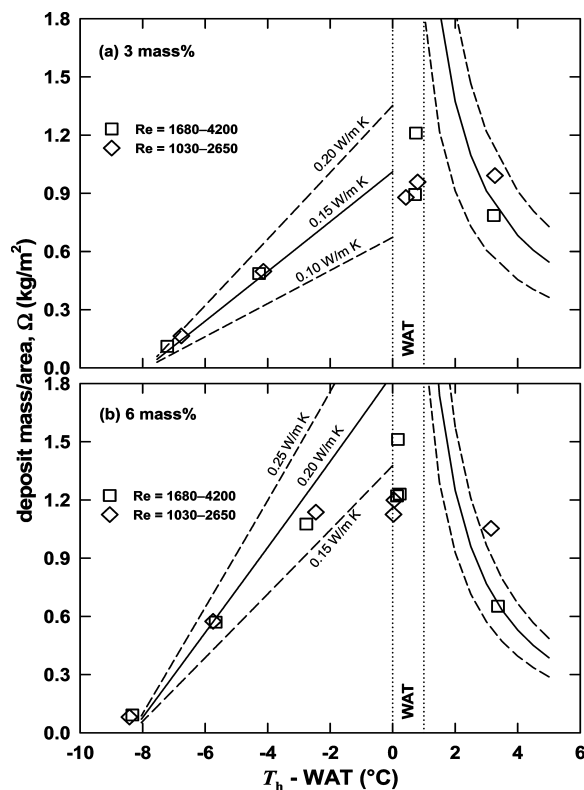


Figure 9. Variation of the deposit mass at coolant temperature of WAT – 10 °C with wax–solvent mixture temperature, T_h , composition and Reynolds number, Re.

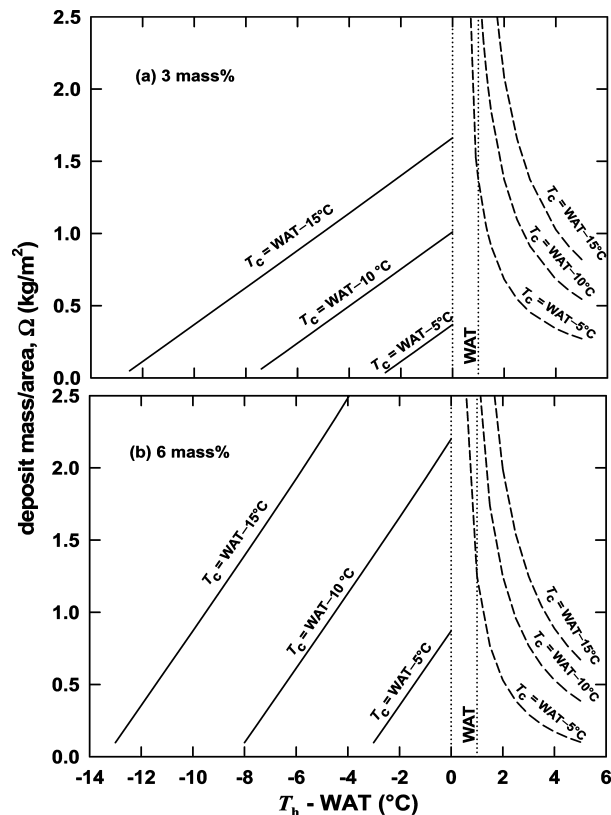


Figure 10. Predictions for the effect of coolant temperature on the deposit mass per unit area.

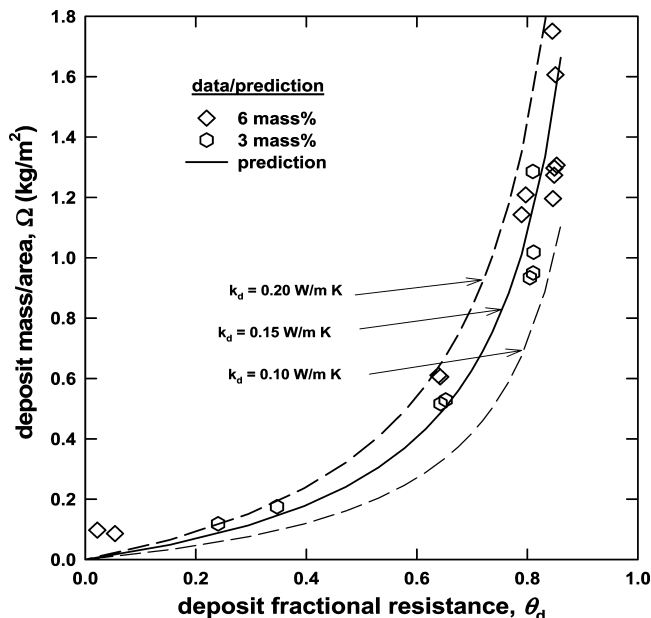


Figure 11. Variation of the deposit mass per unit area, Ω , with the fractional deposit-layer thermal resistance, θ_d .

turbulent conditions.^{17–19,28} This provides further support that the primary mechanism for wax deposition is heat transfer; that is, wax deposition is a thermally driven process under both hot flow and cold flow conditions.

Deposit Compositional Changes during Cold Flow. In Figure 12, the wax composition of analyzed deposit samples, in terms of the carbon number distribution, are compared with those of the initial wax–solvent mixture. These compositional results are presented on a solvent-free (or Norpar13-free) basis and comprise the combined wax composition in the whole deposit including that in both solid and liquid phases.

The results show that the composition of wax constituents in the deposit samples is different from that in the initial wax–solvent mixture. The deposit samples have a higher composition of *n*-alkanes with carbon number greater than C_{29} , whereas the initial wax–solvent mixture has a higher composition of *n*-alkanes with a carbon number lower than C_{29} . It is noted that C_{29} is also the average carbon number of the Parowax sample. Essentially, the deposit samples contain more of the heavier *n*-alkanes than the initial wax–solvent mixture (or Parowax sample). These results suggest that the deposit undergoes an enrichment of wax constituents during the deposition process.

Wax Enrichment Ratio. The deposit wax content includes the fraction of wax in the solid phase of the deposit as well as in the liquid phase trapped within the deposit layer. The wax enrichment ratio, Φ , is defined for comparing the wax content of the deposit with that in the initial wax–solvent mixture:¹⁹

$$\Phi = \frac{\sum_{i=20}^{50} (w_d)_i}{\sum_{i=20}^{50} (w_h)_i} \quad (8)$$

where $(w_d)_i$ is the mass fraction of the *i*th $C_{20}+$ components in the deposit layer, and $(w_h)_i$ is the mass fraction of the *i*th $C_{20}+$ components in the wax–solvent mixture.

Figure 13 shows the effect of the mixture temperature, T_h , on the wax enrichment ratio, Φ , at different Reynolds numbers for cold flow deposition experiments with 6 mass % wax–solvent mixtures. With a decrease in T_h (resulting in a lower deposit mass), the wax enrichment ratio, Φ , is seen to increase slightly.

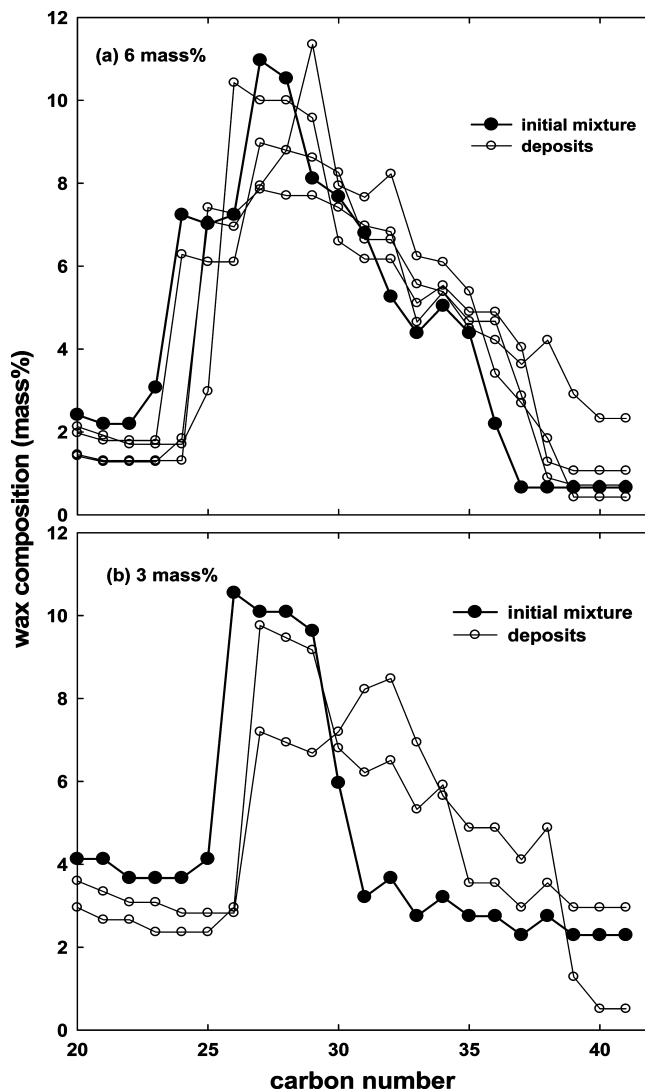


Figure 12. Change in composition of deposit samples from cold flow deposition experiments.

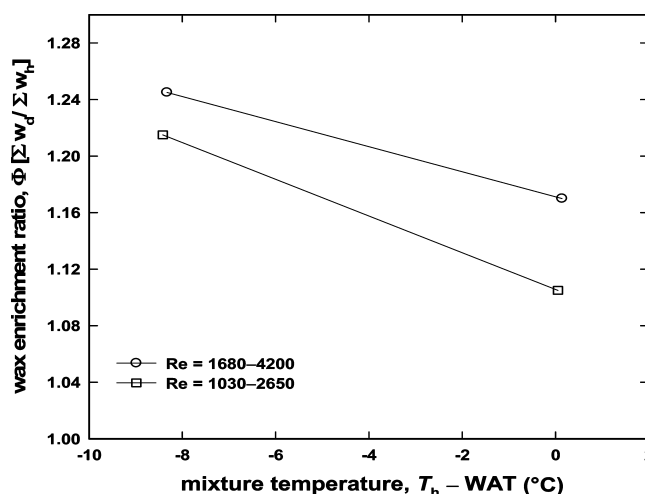


Figure 13. Variation of wax-enrichment ratio, Φ , with mixture temperature (T_h) and Reynolds number (Re) during cold flow deposition with 6 mass % wax–solvent mixtures.

The wax enrichment ratio, Φ , also increased with an increase in the Reynolds number or the flow rate. It is pointed out that, even though the deposit mass did not vary with Re , as shown previously in Figure 9, the wax enrichment ratio, Φ , increased with an increase in Re .

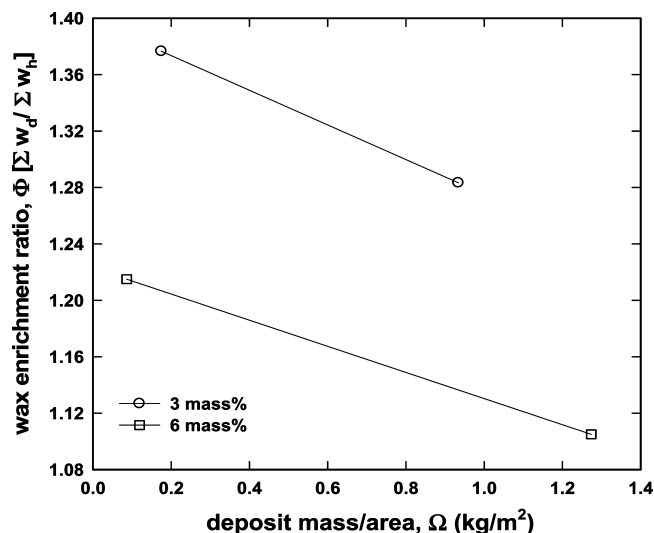


Figure 14. Variation of wax-enrichment ratio (Φ) with deposit mass per unit area (Ω) and mixture composition during cold flow deposition.

Figure 14 shows an interesting relationship between the deposit mass, Ω , and the wax enrichment ratio, Φ . These results, from the cold flow experiments with both mixture compositions, show an increased wax enrichment for a lower deposit mass. That is, the experiments that produced a lower deposit mass also yielded an increased wax enrichment in the deposit. It is also interesting to note that the wax enrichment ratio for the cold flow experiments increased with a decrease in the wax concentration of the wax–solvent mixture.

Significance of Results. The results of this study show that wax deposition could be reduced by first cooling a crude oil or wax–solvent mixture (close to the temperature of the surroundings) before its transportation in a pipeline. The wax deposition can be decreased substantially if the crude oil temperature is brought to slightly above the inner pipe-wall temperature. This might be more economical than maintaining the crude oil temperature under hot flow conditions (i.e., with $T_h > \text{WAT}$) for tackling the deposition problem especially in long pipelines. However, depending on the nature of waxy crude oil, operational problems may be encountered due to an increased apparent viscosity of the slurry created by solid particles suspended in crude oil under cold flow conditions. Effectively, the lowest possible temperature for maintaining cold flow is the PPT.

Our experience from operating the bench-scale flow loop has been that it would be challenging to produce a stable slurry-like mixture from waxy crude oils, particularly with a high PPT such that ($\text{WAT} - \text{PPT}$) is relatively small in magnitude; however, the use of chemical additives for lowering the PPT could be considered. Cold flow might be a suitable deposit prevention method when the ambient temperature is well above the crude oil PPT.

Some of the differences observed between deposition under cold and hot flow include the effects of the mixture temperature and flow rate as well as different deposit thermal conductivities. The results of this study confirm observations made in previous studies, undertaken at hot flow conditions,^{17–19,28,35,36} that the interface temperature, T_d , is equal to the WAT of the liquid phase. During cold flow, the interface temperature, T_d , changed due to the corresponding change in the WAT of the liquid phase (following the precipitation of wax crystals). Thus, the WAT of the liquid phase became lower due to the depletion of waxes, which were crystallized out of the solution and remained suspended. Furthermore, while predictions obtained using the

new parameter, δ_{WAT} , compared well with experimental data, more work is required to fully understand the relationship between the mixture temperature, T_h , and the liquid–deposit interface temperature, T_d (or WAT of the liquid phase), during cold flow. These results, nevertheless, provide a means of estimating wax deposition in a pipeline under conditions of cold flow. The results also provide a framework for determining whether cold flow would be a suitable technique for minimizing wax deposition for a specific waxy crude oil under a given set of operating conditions.

Conclusions

A bench-scale flow-loop apparatus was developed to investigate the deposition of solids from waxy mixtures under cold flow and hot flow conditions. The importance of heat transfer considerations during cold flow deposition was also investigated. The deposition experiments were carried out with two wax concentrations of 3 and 6 mass % using two levels of wax–solvent mixture flow rate, five levels of wax–solvent mixture temperature, and one level of coolant temperature. The deposition process under both cold flow and hot flow was found to be relatively fast, attaining a thermal steady state within about 15 min. An analysis of the deposition data with a steady-state heat transfer model indicated that the deposition process was thermally driven.

Deposition under cold flow conditions was carried out with the wax–solvent mixture flowing as a slurry at a mixture temperature, T_h , lower than the mixture WAT but higher than the PPT. The liquid–deposit interface temperature and deposit thermal conductivity were estimated from the deposition experimental data under both types of flow. The difference between the mixture temperature, T_h , and the liquid–deposit interface temperature, T_d (when $T_h \leq \text{WAT}$) was defined as δ_{WAT} . The δ_{WAT} value was found to be relatively constant with an average value of about 2 °C for all of the cold flow experiments carried out using both wax–solvent mixtures. This supported the supposition that the liquid–deposit interface temperature during cold flow conditions is equal to the lowered WAT of the liquid phase in the flowing wax–solvent mixture. Also, the thermal conductivity of the deposits obtained under cold flow conditions was lower than that of the deposits from hot flow.

The deposit mass during cold flow was found to decrease as the wax–solvent mixture temperature was decreased. Cooling of the wax–solvent mixture to a temperature at which the WAT of the liquid phase became equal to the coolant temperature minimized the solid deposition tendency. An increase in the Reynolds number did not affect the deposit mass. The deposit mass also increased with an increase in the wax concentration in the cold flow experiments. The results agreed well with predictions from a steady-state heat-transfer model. It was shown that a decrease in the coolant or pipe-wall temperature would require further cooling of the wax–solvent mixture to prevent solids deposition. The deposit mass was shown to be related to the fractional thermal resistance offered by the deposit layer at steady state.

The compositional analysis of the deposit samples showed increased fractions of heavier *n*-alkanes and decreased fractions of lighter *n*-alkanes. The wax-enrichment ratio was used as a quantitative measure for comparing the wax content of the deposit with that in the original wax–solvent mixture. The wax-enrichment ratio increased with an increase in the Reynolds number and a decrease in mixture temperature, deposit mass, and wax concentration in mixture.

The results of this study indicate that the deposition under cold flow can be predicted well by heat-transfer considerations. Furthermore, decreasing the waxy crude oil temperature to near ambient or pipe-wall temperature can substantially decrease the deposition tendency, provided the crude oil flow could be maintained. These results provide a framework for further developing the cold flow technology as a viable means for transporting waxy crude oils in a pipeline while minimizing or preventing solids deposition.

Acknowledgment. Financial support from the Natural Sciences and Engineering Research Council of Canada (NSERC) and the Department of Chemical and Petroleum Engineering (Schulich School of Engineering, University of Calgary, Calgary, Alberta, Canada) is gratefully acknowledged. We thank Mr. Bernie Then and Ms. Elizabeth Zalewski for their technical and analytical support.

Nomenclature

a, b, c, d = regression constants in eq 5
 A_i = inside surface area of tube or deposition surface area (m^2)
 b_1, b_2 = regression constants in eq 6
 C_c = average specific heat capacity of the coolant ($\text{J kg}^{-1} \text{K}^{-1}$)
 C_h = average specific heat capacity of the wax-solvent mixture ($\text{J kg}^{-1} \text{K}^{-1}$)
 F_c = volumetric flow rate of the coolant ($\text{m}^3 \text{s}^{-1}$)
 F_h = volumetric flow rate of the wax-solvent mixture ($\text{m}^3 \text{s}^{-1}$)
 h_c = heat transfer coefficient for the coolant ($\text{W m}^{-2} \text{K}^{-1}$)
 h_h = heat transfer coefficient for the wax-solvent mixture ($\text{W m}^{-2} \text{K}^{-1}$)
 k_d = average thermal conductivity of the deposit ($\text{W m}^{-1} \text{K}^{-1}$)
 k_m = average thermal conductivity of aluminum tube ($\text{W m}^{-1} \text{K}^{-1}$)
 L = length of aluminum tube (m)
 \dot{m}_c = mass flow rate of the coolant (kg s^{-1})
 \dot{m}_h = mass flow rate of the wax-solvent mixture (kg s^{-1})
 q = rate of heat transfer at steady state (W)
 q_{gain} = rate of heat gained by the coolant from surroundings (W)
 R_c = thermal resistance of the coolant (K W^{-1})
 R_d = thermal resistance of the deposit layer (K W^{-1})

R_h = thermal resistance of the wax-solvent mixture (K W^{-1})
 R_m = thermal resistance of the aluminum tube wall (K W^{-1})
 r_i = inside tube radius (m)
 r_o = outside tube radius (m)
 Re = Reynolds number
 T_c = average temperature of the coolant ($^{\circ}\text{C}$)
 T_{ci} = inlet temperature of the coolant ($^{\circ}\text{C}$)
 T_{co} = outlet temperature of the coolant ($^{\circ}\text{C}$)
 T_d = liquid-deposit interface temperature ($^{\circ}\text{C}$)
 T_h = average temperature of the wax-solvent mixture ($^{\circ}\text{C}$)
 T_{hi} = inlet temperature of the wax-solvent mixture ($^{\circ}\text{C}$)
 T_{ho} = outlet temperature of the wax-solvent mixture ($^{\circ}\text{C}$)
 T_{wi} = inside wall temperature of aluminum tube ($^{\circ}\text{C}$)
 T_{wo} = outside wall temperature of aluminum tube ($^{\circ}\text{C}$)
 U_i = overall inside heat-transfer coefficient ($\text{W m}^{-2} \text{K}^{-1}$)
 w_d = mass fraction of $\text{C}_{20}+$ n -alkane in the deposit
 w_h = mass fraction of $\text{C}_{20}+$ n -alkane in the wax-solvent mixture
 x_d = deposit layer thickness (m)

Greek Letters

$\delta_{\text{WAT}} = T_h - T_d$ for wax-solvent mixture below WAT ($^{\circ}\text{C}$)
 ρ_d = density of wax-solvent mixture (kg m^{-3})
 θ_c = ratio of coolant (convective) thermal resistance and total thermal resistance
 θ_d = ratio of deposit (conductive) thermal resistance and total thermal resistance
 θ_h = ratio of wax-solvent mixture (convective) and total thermal resistances
 θ_m = ratio of tube-wall (conductive) thermal resistance and total thermal resistance
 Ω = mass of deposit per unit deposition surface area (kg m^{-2})
 Φ = ratio of $\text{C}_{20}+$ n -alkane contents in the deposit and the wax-solvent mixture

Acronyms

PPT = pour point temperature ($^{\circ}\text{C}$)
WAT = wax appearance temperature ($^{\circ}\text{C}$)
WDT = wax disappearance temperature ($^{\circ}\text{C}$)

EF900224R